

GAS DYNAMICS DRIVEN BY THE TWO BARS OF THE MILKY WAY

N.J. Rodríguez-Fernández¹ and F. Combes^{1,2}

Abstract. We present a model of the Milky Way, based on 2MASS star counts, that includes three components: disk, bulge (or large bar) and a small nuclear bar. We have used this mass distribution to obtain an accurate stellar potential and to simulate the gas dynamics of the Galaxy, in particular in the nuclear region. Our dynamical simulations confirm the presence of a nuclear bar. Furthermore, we can constrain the nuclear bar mass. In order to explain the large velocity dispersion of the molecular gas in the nuclear region, the nuclear bar mass should be $(4 - 8) 10^9 M_{\odot}$, i.e., 10-20 % of the bulge mass.

1 Introduction

Studying the morphology and the dynamics of the interstellar gas is necessary to understand some of the processes that govern the evolution of the Galaxy like the large scale star formation, the gas transfer to the nucleus and the fueling of the central super-massive black hole. The Milky Way has four spiral arms and a molecular ring at a radius of 4.5 kpc. From this radius to about 1 kpc, the Galaxy is almost devoid of gas. At 1 kpc there is a ring of HI gas, and inside this ring, in the inner 400 pc there is a nuclear disk where the gas is mainly molecular (see Ferriere et al. 2007 for a summary of the main components of the inner Galaxy). The nuclear disk is assymmetric in Galactic longitude and in velocity. About 75 % of the gas is found at positive longitudes whereas an slightly different 75 % of the gas has positive velocities. Several models have been devoted to the study of the gas dynamics of the Milky Way (Binney et al. 1991, Fux 1999) but none of them has been able to explain the observed characteristics of the nuclear disk.

It is well established that the Milky Way is a barred galaxy but recently, it has been proposed that the Galaxy could also host an small bar in the inner 4 degrees (Alard 2001, Nishiyama et al. 2005). In order to investigate the gas dynamics in the presence of two bars, we have modelled the 2MASS star counts maps of Alard (2001) to derive the mass distribution of the Milky Way. Using this mass distribution, we have calculated a realistic potential and we have done numerical simulations of the gas dynamics.

2 Modeling the star counts

Figure 1 shows the 2MASS star counts map of Alard (2001). We have modeled this map using a star density distribution given by three components: a triaxial bulge or large bar, an exponential disk and a small nuclear bar. We have chosen an exponential disk as defined by Wainscoat et al. (1992), with vertical and radial scale parameters h_z and h_r , respectively. The COBE and 2MASS data show clearly the *boxy* nature of the Galactic bulge. Therefore, we have adopted a triaxial *boxy* Gaussian to represent the bulge (function G2 of Dwek et al. 1995). The free parameters of this function are the characteristic scale along each symmetry axis (x_0, y_0, z_0) , a normalization factor ρ_0 , and the angle that gives the orientation of the long axis with respect the line of sight α^B . Angles are measured clockwise with respect to the sun-Galactic center line. In contrast to the bulge, the small nuclear bar found by Alard does not seem to be boxy. Therefore we have taken a triaxial Gaussian function to represent this component (function G1 of Dwek et al. 1995):

$$\rho^b(x, y, z) = \rho_0 \exp(-0.5r^2) \quad \text{with} \quad r = \left[\left(\frac{x - x_1}{x_0} \right)^2 + \left(\frac{y}{y_0} \right)^2 + \left(\frac{z}{z_0} \right)^2 \right]^{1/2} \quad (2.1)$$

¹ IRAM, 300 rue de la Piscine, 38406 Saint Martin d'Herès, France

² Observatoire de Paris, LERMA, 61 Av. de l'Observatoire, 75014 Paris, France

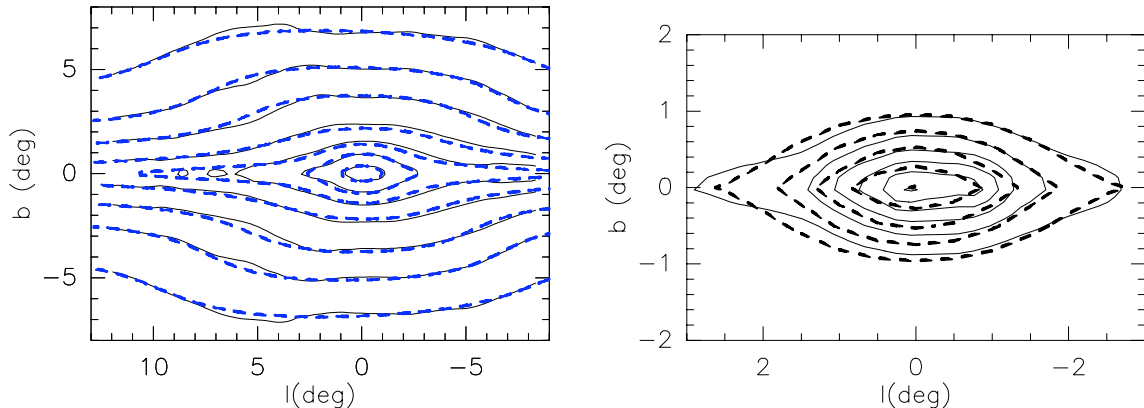


Fig. 1. Thin solid contours represent the star counts map of Alard (2001). Thick dashed lines are the best fit obtained with a star counts model with $\alpha^B = 80$ deg, $h_r = 2.5$ kpc and $\alpha^b = 120$ deg. The panel on the right is a zoom of the nuclear region.

Table 1. Results of the fits to the star counts data using disk, bulge and nuclear bar. The parameters of the bulge and the disk are: $\alpha^B = 80$, $x_0^B = 1.117$, $y_0^B = 0.513$, $z_0^B = 0.362$ $h_r = 2.5$, $h_z = 0.153$. The bar angle α^b is also fixed, the other parameters are free and used to obtain the best fit to the data

Bulge ρ_0^B	Disk ρ_0^D	Bar					χ^2
		x_0^b kpc	y_0^b kpc	z_0^b kpc	ρ_0^b	α^b deg	
0.381E-02	0.255E-03	0.161	0.130	0.097	0.153E+00	0.0	0.357
0.381E-02	0.256E-03	0.161	0.130	0.097	0.151E+00	15.0	0.358
0.383E-02	0.255E-03	0.215	0.138	0.092	0.110E+00	120.0	0.350
0.381E-02	0.255E-03	0.161	0.130	0.097	0.151E+00	165.0	0.357

where x_0, y_0 and z_0 are the characteristic sizes along each symmetry axis, x_1 is a parameter that allows to fit a lopsided bar, and ρ_0 is a global normalization factor. The orientation of this bar is given by an angle α^b which in principle is different to the angle that defines the orientation of the bulge (α^B).

First, we have fitted a reduced data set (without the nuclear region) using only disk and bulge for fixed values of the bulge angle ($\alpha^B = 30, 45, 55, 70, 80, 90$ deg) and the disk radial scale ($h_r = 1.5, 2, 2.5, 3.5$ kpc). For all α^B 's, the best fits are always obtained with $h_r = 2.5$ kpc. This is in agreement with the radial scale length of the disk derived from previous studies in the infrared (Lopez-Corredoira et al. 2005, Freudenreich 1998). Regarding the angle of the bulge, the best fit is obtained for 80 deg, although χ^2 is only a 2.8 % higher for $\alpha^B = 70$ deg. This is also in agreement with other studies of the structure of the inner Galaxy which give angles in the range 50-81 deg (Dwek et al. 1992, Freudenreich 1998). The axis ratios of the bulge is $x_0/x_0 : y_0/x_0 : z_0/x_0 = 1 : 0.5 : 0.3$ and it is also in perfect agreement with those derived by Lopez-Corredoira et al. (2005). In a second step we have fixed the nuclear bar parameters and we have fitted all the data using also the nuclear bar. Table 1 gives the nuclear bar parameters of the best fits for $\alpha^B = 80$ deg. The best fits are found for $\alpha^b = 120$ deg for all the α^B 's. Good fits are also obtained with α^b close to 0 deg (nuclear bar perpendicular to the line of sight). Figure ?? shows the best fit with $\alpha^B = 70$ deg and $\alpha^b = 120$. Fitting a lopsided bar, one gets $x_1 = 20$ pc, which for the best fit, is about 10 % of the semi-major axis.

3 Simulations of the gas dynamics

Using the mass distribution determined from the fits to the 2MASS data, we have computed a realistic potential by standard FFT techniques. To obtain global scaling factors to account for the total mass of the Galaxy, we have compared the computed rotation curve with the measured rotation curve (Clemens 1985). To have a flat

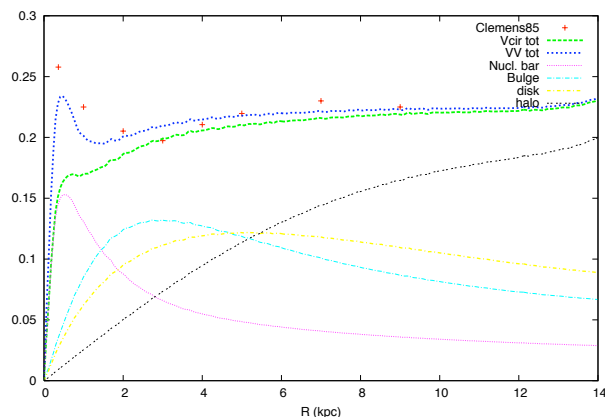


Fig. 2. Red crosses represent the rotation curve determined by Clemens (1985). The blue curve is the rotation curve computed from our mass model for $\alpha^B = 70$ deg and $\alpha^b = 120$ deg. The green curve is the rotation curve computed only with the axi-symmetric part of the potential. The other curves represent the contribution of the bulge, disk, nuclear bar and halo to the total rotation curve.

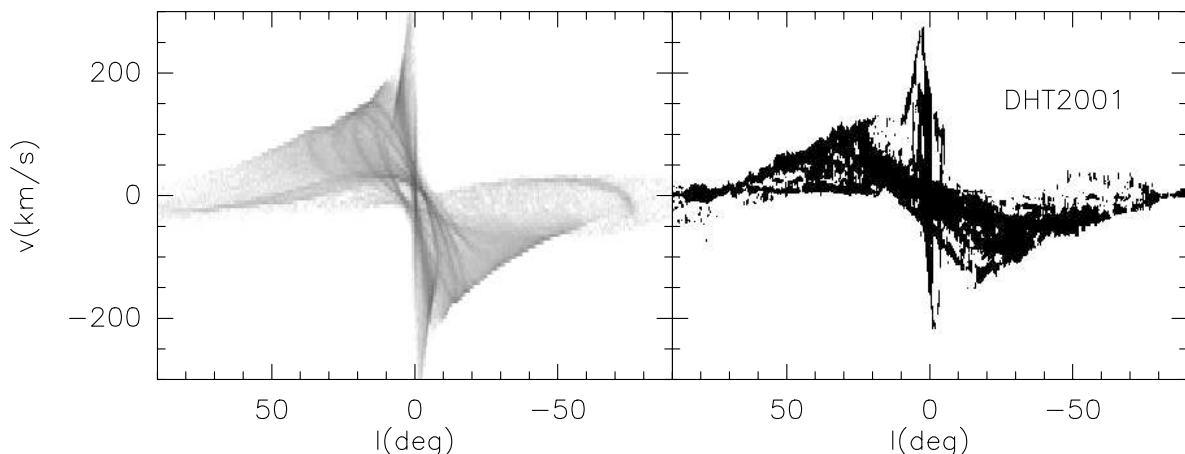


Fig. 3. Right panel: longitude-velocity diagram of the CO(1-0) emission (Dame et al. 2001). Left panel: longitude-velocity diagram of our simulation for $\alpha^B = 80$ deg and $\alpha^b = 120$ deg with $\Omega_p = 45 \text{ km s}^{-1} \text{ kpc}^{-1}$

rotation curve at large radii we have added a massive halo. Figure 2 shows the modeled rotation curve obtained with the results of the best fits for $\alpha^B = 70$ deg and $\alpha^b = 120$ deg and total masses of the different mass components: $M^D = 6.3 \cdot 10^{10} M_\odot$, $M^B = 4.0 \cdot 10^{10} M_\odot$ and $M^b = 8.3 \cdot 10^9 M_\odot$.

We have used the code of Combes & Gerin (1985) to simulate the movement of gas clouds in this stellar potential. In the current version of our models, the bulge and the nuclear bar rotate with the same angular speed Ω_p . The effects of the gas self-gravitation are neglected. The clouds move as test particles except when they collide inelastically. The relative velocity of two collisions partners loses 60% of its absolute value in the collision. A detailed discussion of the collisional schema can be found in Combes & Gerin (1985).

Figures 3 and 4 show the longitude-velocity diagram and the face on view of the simulation for $\alpha^B = 80$ deg and $\alpha^b = 120$ deg with a pattern speed $\Omega_p = 45 \text{ km s}^{-1} \text{ kpc}^{-1}$. The right panel in Fig. 3 also shows the longitude-velocity diagram obtained with the CO(1-0) data of Dame et al. (2001). The positions of the spiral arms of the Galaxy as derived from observations of HII regions (Georgelin & Georgelin 1976) are showed by dashed lines in the left panel of Fig. 4. The simulations reproduce the main features of the observations as the position and curvature of the spiral arms (Fig. 4). This is also shown in Fig. 3, where the tangent point of the Carina arm at $l \sim 80$ deg is nicely reproduced by the simulations. Indeed, to reproduce the pitch angle of the spirals and the locus of the Carina arm in the longitude velocity diagram, the pattern speed of the potential

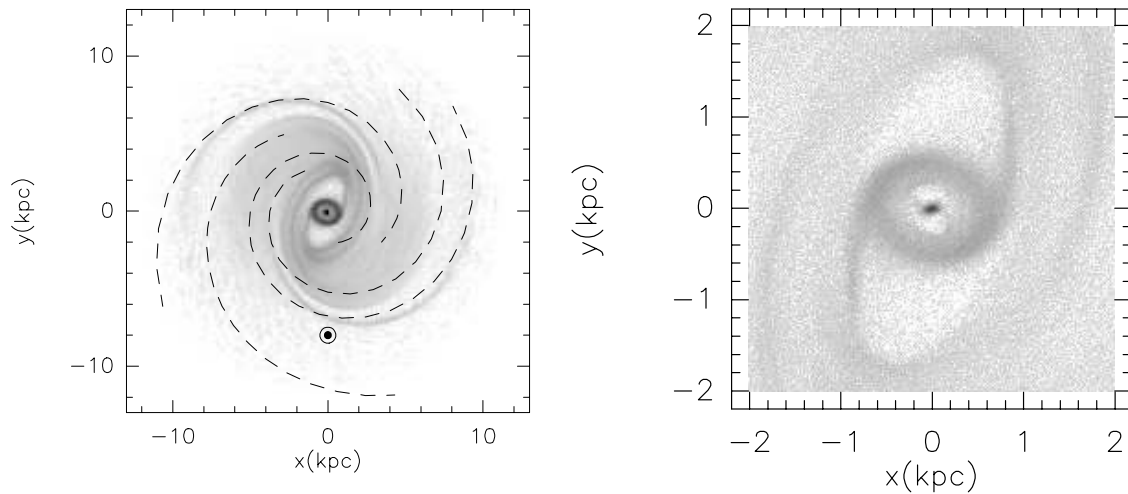


Fig. 4. Face on view of the simulation shown in Fig. 3. The dashed lines trace the position of the spiral arms inferred from the observations of HII regions by Georgelin & Georgelin 1976. The position of the sun at (0,-8) is also shown.

(Ω_p) has to be $45 \text{ km s}^{-1} \text{ kpc}^{-1}$. From our simulations the angle of the bulge with respect to the Sun-Galactic Center line must be in the range 10-45 deg.

The right panel of Fig. 4 shows the face on view of the inner 4 kpc. The gas morphology is dominated by the so-called off-axis shocks along the bar. These structures are connected to a ring with a radius of $\sim 1 \text{ kpc}$, which corresponds to the observed HI ring (Ferriere et al. 2007). In the inner 400 pc there is a central accumulation of gas that corresponds to the molecular nuclear disk. In the simulations, the nuclear disk is connected to the HI ring by an small spiral with two arms. The morphology down to a radius of 1 kpc is almost independent of the position angle of the nuclear bar. No signatures are found at this scale of the possible lopsideness of the nuclear bar. However, the mass of the nuclear bar can be well constrained. To reproduce the huge velocity dispersion of the nuclear disk observed in the longitude-velocity diagram, the mass of the nuclear bar has to be $M^b = (4 - 8) 10^9 M_\odot$, *i.e.*, 10-20 % of the mass of the bulge.

References

- Alard, C. 2001, A&A, 379, L44
 Binney, J., Gerhard, O. E., Stark, A. A., Bally, J., & Uchida, K. I. 1991, MNRAS, 252, 210
 Clemens, D.P., 1985, ApJ 295, 422
 Combes, F. and Gerin, M., 1985, A&A 150, 327
 Dame, T. M., Hartmann, D., & Thaddeus, P. 2001, ApJ, 547, 792
 Dwek, E., Arendt, R.G., Hauser, M.G. et al., 1995, ApJ 445, 716
 Ferrière, K., Gillard, W., & Jean, P. 2007, A&A, 467, 611
 Freudenreich, H. T. 1998, ApJ, 492, 495
 Fux, R. 1999, A&A, 345, 787
 Georgelin, Y. M., & Georgelin, Y. P. 1976, A&A, 49, 57
 López-Corredoira, M., Cabrera-Lavers, A., & Gerhard, O. E. 2005, A&A, 439, 107
 Nishiyama, S., et al. 2005, ApJL, 621, L105
 Wainscoat, R.J., Cohen, M., Volk, K., et al., 1992 ApJS, 83 ,11